Prediction of Stress in Radiation Therapy: Integrating Artificial Intelligence with Biological Signals

Sangwoon Jeong , Hongryull Pyo , Won Park , Youngyih Han *

Posted Date: 11 January 2024

doi: 10.20944/preprints202401.0941.v1

Keywords: radiation oncology; artificial intelligence; biological signals; physiological stress; heart rate variability; machine learning

Article

Prediction of Stress in Radiation Therapy: Integrating Artificial Intelligence with Biological Signals

Sangwoon Jeong [1], Hongryull Pyo [2,3], Won Park [2,3] and Youngyih Han [1,2,3,*]

[1] Department of Health Sciences and Technology, SAIHST, Sungkyunkwan University, Seoul, 06355, Korea; sharkj@skku.edu
[2] Department of Radiation Oncology, Samsung Medical Center, Seoul, 06355, Korea.
[3] School of Medicine, Sungkyunkwan University, Seoul, 06355, Korea.
* Correspondence: youngyih@skku.edu.

Simple Summary: Patients undergoing radiation therapy can experience stress because of the fear of treatment. Stress causes muscles to contract, which can reduce the accuracy of the patient setup. In this study, we used biological signals to identify and artificial intelligence to predict stress during radiation therapy. Stress was calculated by analyzing biological signals measured before and during radiation therapy. We used various artificial intelligence models to verify the models optimized for stress prediction. Our findings indicate that over 90% of patients experience stress during treatment and artificial intelligence can predict this stress with over 80% accuracy. This study is pivotal for identifying patients requiring stress reduction before therapy, potentially enhancing the precision of cancer radiation therapy.

Abstract: Stress can reduce the accuracy of radiation therapy owing to muscle contraction and changes in breathing patterns. This study aimed to predict stress in patients before each treatment session using artificial intelligence (AI) from biological signals to enhance treatment accuracy. We measured 123 stress cases in 41 patients and calculated stress scores by analyzing seven stress-related features derived from heart rate variability obtained from photoplethysmography. The study analyzed stress score distribution and observed its trend changes throughout the treatment. Before-treatment information was used to predict changes in stress features during treatment. AI models included both non-pre-trained (Decision Tree, Random Forest, Support Vector Machine, Long Short-Term Memory (LSTM), Transformer) and pre-trained (ChatGPT) models. The performance was evaluated using 10-fold cross-validation, exact match ratio, accuracy, recall, precision, and F1 score. More than 90% of the patients experienced stress during radiation therapy. From all the classifications, LSTM and prompt engineering GPT4.0 had the highest accuracy (feature classification, LSTM: 0.703, GPT4.0: 0.659, stress classification: LSTM: 0.846, GPT4.0: 0.769). Our research pioneers the use of AI and biological signals for stress prediction in radiation therapy, potentially identifying patients needing psychological support, and suggesting methods to improve radiotherapy effectiveness through stress management.

Keywords: radiation oncology; artificial intelligence; biological signals; physiological stress; heart rate variability; machine learning

1. Introduction

Overcoming cancer, a leading cause of death worldwide is a challenge for global health [1]. Various treatment modalities, such as chemotherapy, immunotherapy, hormonal therapy, surgery, and radiation therapy, are used alone or in combination to treat cancer [2, 3]. The role of radiation therapy has been increasing owing to the non-invasive characteristics that is feasible for elderly patients and the technical advancement of treatment techniques focusing radiation on targeted tumors.

A necessary procedure in radiation therapy involves the creation of an individual treatment plan to focus high-energy radiation on the tumor while sparing nearby critical organs, using simulation computed tomography images. For successful radiation therapy, the accurate positioning of the patient, identical to that in the treatment plan, is essential. If the patient's position does not match the treatment plan, the therapeutic effect is reduced and damage to normal tissues can occur [4-6]. For

 doi:10.20944/preprints202401.0941.v1

head and neck cancer, a positioning error of even 3 mm can reduce the dose to the tumor by as much as 10% [7]. Similarly, in cervical cancer, a rotational error of 1° can result in a 2% reduction in the tumor dose and an 11% increase in the dose to nearby organs at risk [8]. Therefore, accurate beam alignment in accordance with the treatment plan to patients is critical for optimizing the therapeutic outcomes.

Accuracy of radiation treatment is influenced by both technological and human factors [9]. Technological uncertainties encompass mechanical issues with radiation therapy equipment, such as imprecision in the leaf position, beam output, and beam profiles, which are typically addressed through regular quality assurance procedures [10, 11]. Human factors, such as respiratory and gastrointestinal motion, shrinkage of the targeted tumor volume, and patient stress (anxiety) play significant roles [12-14]. The inherent variability in human respiratory and digestive system movements can cause unpredictable displacements of the body and internal organs, which can be mitigated using techniques such as gating, tumor tracking, and image-guided radiation therapy [15]. The treatment plan was modified using adaptive radiotherapy to accommodate the shrinkage of the target volume [16, 17]. Although various methods to counteract these factors are used in daily patient treatment and are under development, there is a noticeable scarcity of research addressing the impact of patient stress on radiation therapy.

Psychological stress triggers the sympathetic nervous system, leading to physiological changes such as increased heart rate (HR), blood pressure, breathing rate, and muscle stiffness [18-21]. Stress-induced muscle stiffness can compromise the precision of patient positioning in setting up daily radiation treatment. Assessment of stress levels in the general population is commonly conducted through surveys [22, 23], and this methodology extends to studies examining stress in patients undergoing medical treatment [24]. During the pandemic, the decline in mental health and quality of life of patients with cancer was assessed through a survey [25], and the stress of patients with benign prostatic hyperplasia was confirmed through a survey [26]. Although survey research can efficiently yield data, the reliability of self-reported information is a subject of concern [27]. Consequently, a growing body of research has focused on the measurement of stress through biological signals, which may offer more objective data points than self-reported surveys.

Evaluation of stress through biological signal monitoring is an emerging and pivotal field of medical research. This approach encompasses a variety of metrics, including photoplethysmogram (PPG), electrocardiogram (ECG), body temperature, respiratory patterns, vocal properties, and electroencephalogram (EEG), each offering unique insights into the physiological manifestations of stress [28-30]. Under stress, the sympathetic nervous system triggers an increase in body temperature and alters the respiratory dynamics to a faster and shallower pattern. Vocal attributes change noticeably under stress, typically resulting in higher pitch and greater variability. Additionally, EEG recordings revealed an increase in beta wave activity during stress. Two of the most significant indicators in this field are PPG and ECG, both of which monitor changes in blood flow. Changes in blood flow are instrumental in determining heart rate variability (HRV), a key metric in stress evaluation [31, 32]. The reliability and utility of HRV as a stress measure have been substantiated by comparison with traditional stress surveys [33]. Moreover, the integration of HRV analysis into wearable technologies such as smartwatches, has opened new avenues for real-time, noninvasive stress monitoring [34]. Hence, HRV analysis is a promising alternative to survey-based methods that offer a more objective and continuous assessment of stress levels.

Stress in patients undergoing radiation therapy has been identified in survey studies [35, 36]. It is observed that a majority of these patients experience heightened stress levels, particularly in the initial stages of their treatment. This underscores the need for effective stress-management strategies. However, implementing universal stress-reduction measures for all patients can be resource-intensive and requires additional manpower and time. To address this challenge, we leveraged Artificial Intelligence (AI) techniques in conjunction with biological signal analysis to identify patients who are susceptible to stress during radiation therapy. Our approach involved training machine learning models on HRV data collected both before and during the treatment sessions. This study aimed to use before-treatment HRV data to predict the likelihood of patients experiencing

 doi:10.20944/preprints202401.0941.v1

significant stress during therapy sessions. This prediction enables us to tailor stress management interventions more effectively by focusing on those who need them the most.

2. Materials and Methods

2.1. Patients

The study protocol, including patient recruitment and data collection methods, was approved by the Institutional Review Board of the Samsung Medical Center (IRB number 2020-11-162). Prior to enrollment, written informed consent was obtained from all participants, confirming their voluntary participation and understanding of the study's aims and processes. Our study prospectively enrolled patients who underwent radiation therapy for lung cancer. The recruitment period spanned from December 2020 to November 2023. The inclusion criteria were carefully defined to ensure a representative and relevant patient cohort. These criteria included (1) adult patients (aged < 80 years) receiving radiation therapy for the first time to capture initial stress responses untainted by previous experiences; (2) patients capable of effective communication, ensuring accurate self-reporting and feedback regarding the study procedures and their well-being; and (3) patients who could comfortably wear the sensor without experiencing discomfort, as any discomfort could confound stress measurements. The patient recruitment process is illustrated in Figure 1. Initially, 238 patients were approached for participation in this study. Of these, 79 consented to participate, reflecting a 33% response rate. During the study, certain patients were excluded due to reasons such as discomfort while wearing the sensor, discontinuation of radiation therapy, or data errors from sensor malfunction. These exclusion criteria helped to maintain the integrity and reliability of the collected data. To ensure the privacy and confidentiality of the participants, all collected data were anonymized. Identifiable information was removed and replaced with unique codes, thereby securing patient privacy and adhering to ethical data-handling practices.

Preprints (www.preprints.org) | NOT PEER-REVIEWED | Posted: 11 January 2024 doi:10.20944/preprints202401.0941.v1

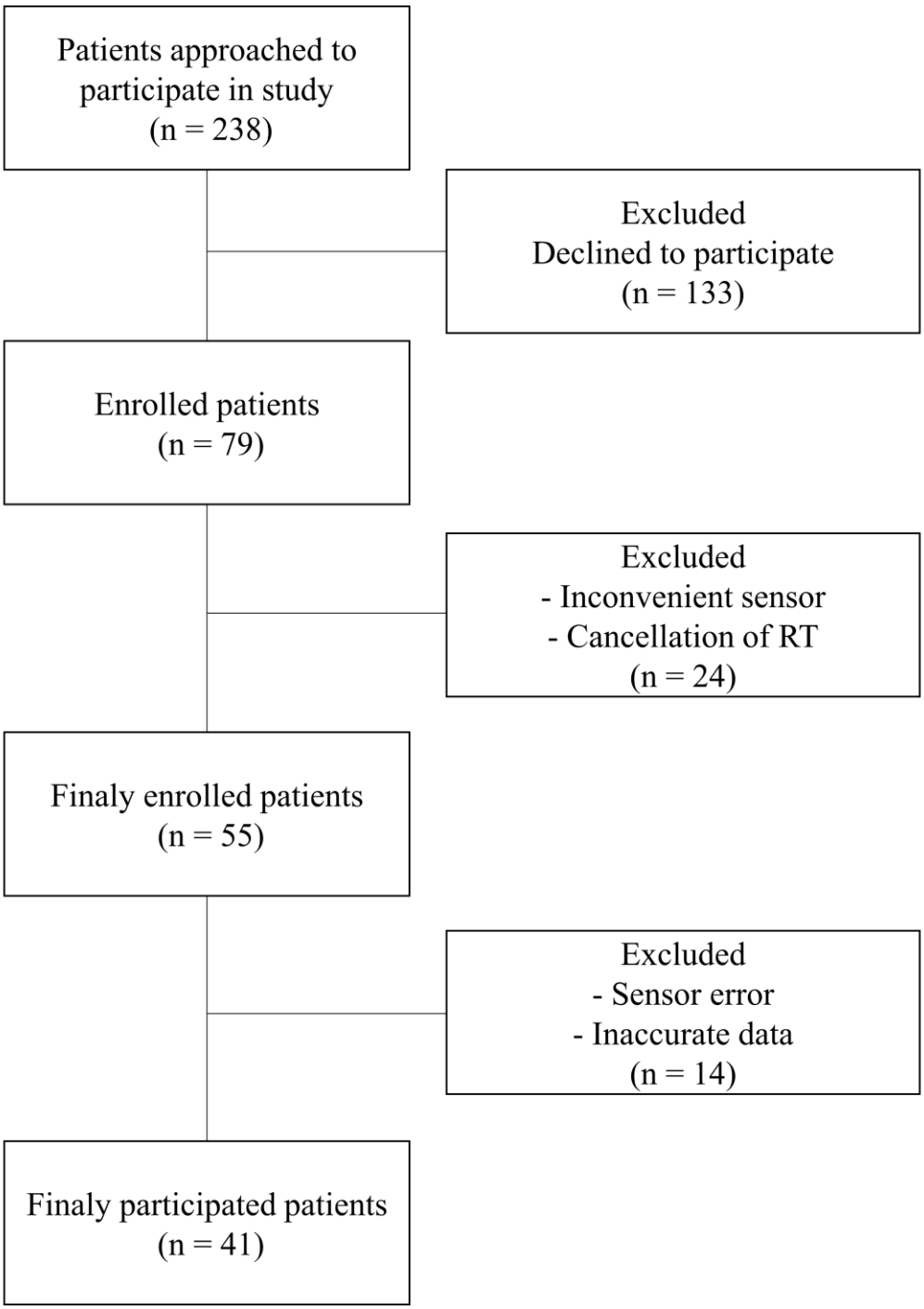

Figure 1. Flowchart of patient enrollment.

2.2. Data acquisition and processing

Data collection commenced with patients wearing a biological sensor (Laxtha, Ubpulse 360, Daejeon, Korea) upon arrival in the waiting room prior to receiving radiation therapy. The sensor was positioned on the finger to ensure no interference during the treatment procedure. After a 10-minute acclimatization period, patients were escorted to the treatment room, where they continued to wear the sensor throughout their radiation treatment session. Upon completion of the treatment, the sensor was returned, and the collected PPG data were securely transferred to a dedicated computer system for analysis. Signals arising from patient movements and those resulting from sensor errors were carefully removed to ensure data integrity. To analyze stress changes during treatment, a minimum of one day and a maximum of five day's data were extracted for each patient. Subsequently, the PPG data were segmented into two distinct phases for analysis: the before-

 doi:10.20944/preprints202401.0941.v1

treatment phase, captured while the patient was in the waiting room, and the during-treatment phase, recorded when the patient lay on the treatment couch. To account for potential HR elevations due to movement, we isolated 5 min of data following a 2-minute stabilization period in both the before- and during-treatment phases. From these phases, the HRV was computed by analyzing the intervals between successive PPG peaks. Preprocessing of the PPG data and subsequent HRV analyses were conducted using MATLAB R2020b (MATLAB, MathWorks, Natick, MA, USA) to ensure a standardized and reproducible methodology.

2.3. Stress features

Identification and accurate quantification of stress features are important for the assessment of stress levels using HRV analysis. In this study, we operationalized stress using a set of physiological markers derived from PPG signals. The second derivative of the PPG signal was used to pinpoint the heartbeat peaks, and HRV was calculated by measuring the intervals between these peaks. The selection of HRV-related stress features was based on a comprehensive literature review, identifying seven features consistently associated with physiological stress responses [37-47]. These features were HR, Standard deviation of NN intervals (SDNN), square root of the mean sum of squares of successive NN interval differences (RMSSD), percentage of successive NN intervals differing by more than 50 ms (pNN50), power of high-frequency range (HF), ratio of low-frequency range/high-frequency range (LF/HF), and total power of frequency range (TP). Under stable conditions, stress was typically indicated by increased HR and LF/HF, whereas SDNN, RMSSD, pNN50, HF, and TP were decreased (Table 1). We employed these stress features to calculate the stress score (range: 0-100%) by observing changes before and during treatment.

Table 1. Summary of stress-related features based on heart rate variability.

Features	Unit	Description	Stressful
HR	bpm	Average number of heartbeats per minute	Increase
SDNN	ms	Standard deviation of NN intervals	Decrease
RMSSD	ms	Square root of the mean sum of squares of successive NN intervals differences	Decrease
pNN50	%	Percentage of successive NN intervals differing more than 50 ms	Decrease
HF	ms^2	Power of high-frequency range (0.15 – 0.4 Hz)	Decrease
LF/HF	ms^2	Ratio low-frequency range / high-frequency range	Increase
TP	ms^2	Total power of frequency range (0.004 – 0.4 Hz)	Decrease

2.4. Stress prediction

Predicting patient stress in the waiting room before treatment is crucial to enhance the accuracy of setting up patients for radiation treatment. This enables the early implementation of measures to reduce stress, potentially improving treatment efficacy. Non-pretrained and pretrained models were used for stress prediction. The non-pretrained model categories include decision tree (DT) [48], random forest (RF) [49], support vector machines (SVM) [50], long short-term memory (LSTM) [51], and transformer [52]. The pre-trained models used were OpenAI's ChatGPT, which is based on a Large Language Model (LLM) and enables prompt engineering and fine-tuning. Prompt engineering involves the strategic design of input prompts to elicit the desired responses from an LLM [53], whereas fine-tuning refers to the process of adjusting an LLM's parameters on a specific dataset to improve its performance for particular tasks [54]. The non-pretrained models were assessed using 10-fold cross-validation to evaluate their ability to handle eight different input datasets (Type 1, only before-treatment features; Type 2, before-treatment features with age; Type 3, before-treatment features with sex; Type 4, before-treatment features with day; Type 5, before-treatment features with age and sex; Type 6, before- treatment features with age and day; Type 7, before-treatment features with sex and day; and Type 8, before-treatment features with age, sex, and day). These datasets included treatment day, age, sex, and seven stress features identified before treatment. The model

Preprints (www.preprints.org) | NOT PEER-REVIEWED | Posted: 11 January 2024 doi:10.20944/preprints202401.0941.v1

outputs were designed to classify the predicted changes in stress features during treatment (Figure 2). Subsequently, the top three input datasets from the performance of the non-pretrained models were selected for further analysis with the pretrained models. The pretrained model was evaluated against a representative one-fold out of a 10-fold cross-validation of the non-pretrained model. Therefore, the pretrained and non-pretrained models compared the results of the one-fold dataset. The pretrained models performed prompt engineering in GPT-3.5 and GPT-4.0 and fine-tuning in GPT-3.5-turbo-1106.

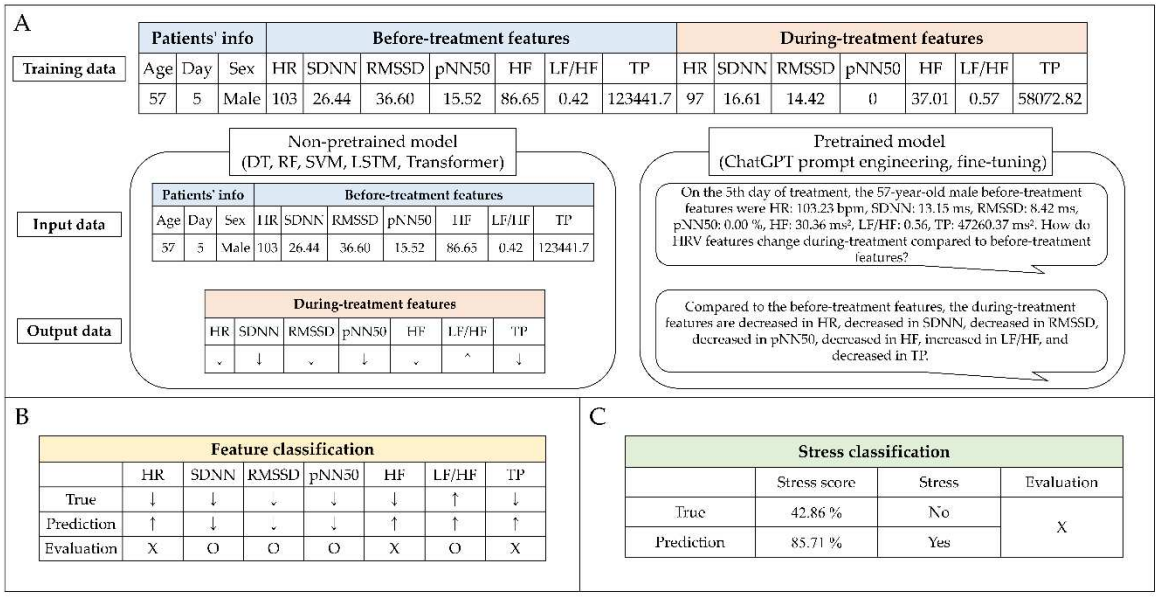

Feature classification	HR	SDNN	RMSSD	pNN50	HF	LF/HF	TP
True	↓	↓	ˇ	↓	↓	↑	↓
Prediction	↑	↓	ˇ	↓	↑	↑	↑
Evaluation	X	O	O	O	X	O	X

Figure 2. Stress prediction workflow using artificial intelligence. (A) The training process of non-pretrained model and pretrained model. (B) Feature classification evaluation process. (C) The stress classification evaluation process based on 50% of the stress score calculated using the results of feature classification.

2.5. Evaluation

A comprehensive evaluation of our predictive models involved several statistical and machine learning metrics to assess the stress score distribution and its variation throughout the treatment course. We analyzed the aggregated stress score changes and classified them by sex to observe potential differences in stress patterns between male and female patients over a period of up to four days. The non-parametric Wilcoxon signed-rank test was employed for paired comparisons, whereas the Friedman test was used to analyze changes across multiple-day trends. The Mann-Whitney U test was used to compare stress scores between males and females.

To assess the predicted stress features during treatment, we adopted two analytical approaches: feature classification (multi-label) and stress classification (binary). Feature classification utilized the raw output from our models to evaluate prediction accuracy across multiple labels. The key metrics included the Exact Match Ratio (EMR) and standard classification metrics such as accuracy, recall, precision, and F1 score, providing a holistic view of the models' performance. The feature classification result is calculated as a stress score but the stress classification is classified as “yes (> 50%)” or “no (< 50%)” based on the criterion of a stress score of 50%. The effectiveness of the stress classification was quantified using accuracy, recall, precision, and F1 score.

The non-pre-trained models were developed using Python (version 3.7.16) with traditional machine learning algorithms, such as DT, RF, and SVM, implemented via the Scikit-learn library (version 1.3.2). Deep learning algorithms, such as LSTM and Transformer, were operationalized using Pytorch (version 1.7.1), and all computations were performed on an NVIDIA GeForce 2080Ti GPU. The Scikit-learn library was utilized to compute various performance metrics to ensure consistency and reliability in our evaluation methodology.

 doi:10.20944/preprints202401.0941.v1

3. Results

3.1. Patient characteristics

Our study enrolled 41 patients, comprising 27 males (65.85%) and 14 females (34.15%) with a mean age of 67.15 years (interquartile range: 47.0–80.0 years). Table 2 presents a detailed summary of the characteristics of the enrolled patients, including sex distributions and age ranges. Regarding stress analysis, we observed 123 cases of stress measurements over the course of the study. Of these, 12 were identified without stress indicators, representing a stress-free state. The most frequently observed stress score was 85.71% (n = 26). The stress was recorded for up to 14 days. However, from the fifth day onwards, the number of stress cases recorded each day was less than 10.

Table 2. Characteristics of enrolled patients.

Characteristic	N	(%)
All patients	41	(100)
Sex		
Male	27	(65.85)
Female	14	(34.15)
Age		
All	Mean, 67.15	(Range, 47 – 80)
Male	Mean, 66.56	(Range, 47 – 80)
Female	Mean, 68.29	(Range, 57 – 80)
Stress case		
All	123	(100)
Male	81	(65.85)
Female	42	(35.15)
Stress score		
0 %	12	(9.76)
14.29 %	18	(14.63)
28.57 %	18	(14.63)
42.86 %	17	(13.82)
57.14 %	6	(4.88)
71.43 %	17	(13.82)
85.71 %	26	(21.14)
100 %	9	(7.32)
Stress case day		
1	17	(13.82)
2	18	(14.63)
3	22	(17.89)
4	20	(16.26)
5 - 14	46	(37.40)

3.2. Stress score changes as treatment progresses

Using data from days one to four, when more than 15 stress cases were obtained, we confirmed the change in stress score over time (Figure 4). There were no differences by date or overall trends in the all, male and female data. Although the trend over treatment was not significant, stress scores

Preprints (www.preprints.org) | NOT PEER-REVIEWED | Posted: 11 January 2024 doi:10.20944/preprints202401.0941.v1

increased in males and decreased in females. The difference in stress scores between males and females on day four was significant (p = 0.0384) (Table 3).

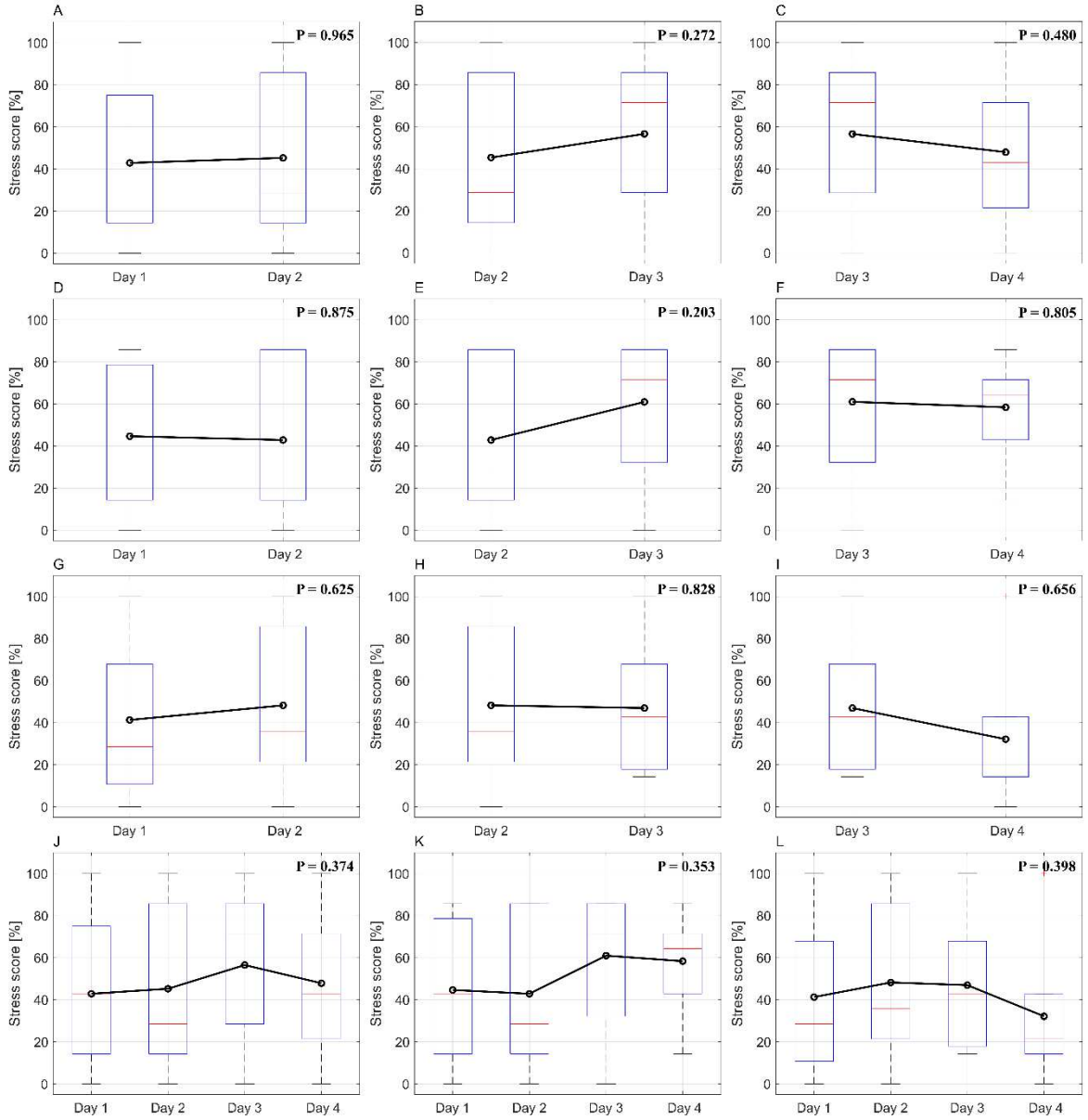

Figure 3. Compare stress score changes by date and check overall trends. (A) ~ (C) Comparison of changes in stress score of all patients for each day. (D) ~ (F) Comparison of changes in stress score of male patients for each day. (G) ~ (I) Comparison of changes in stress score of female patients for each day. (J) Analysis of stress score change trends for all patients and all dates. (K) Analysis of stress score change trends for all days of male patients. (L) Analysis of stress score change trends for all days of female patients.

Table 3. Stress scores of males and females on each day.

	Day 1	Day 2	Day 3	Day 4
Male	44.69 ± 33.70 %	42.90 ± 35.67 %	61.01 ± 29.83 %	58.39 ± 22.37 %
Female	41.31 ± 39.45 %	48.26 ± 37.40 %	46.99 ± 31.67 %	32.17 ± 31.28 %
P-value	0.8707	0.6691	0.2978	0.0384

Preprints (www.preprints.org) | NOT PEER-REVIEWED | Posted: 11 January 2024 doi:10.20944/preprints202401.0941.v1

3.3. Non-pretrained model features classification

In our analysis, we utilized stress case data to classify the treatment features using non-pretrained models across eight different input datasets. The average results of the 10-fold cross-validation are summarized in Table 4. In terms of the EMR, the LSTM model using the type 8 dataset performed the best, achieving an EMR of 0.172. However, the RF model exhibited superior performance across all other datasets. Regarding the accuracy, the LSTM model with the type 7 dataset had the highest accuracy of 0.699. Moreover, the LSTM model had the highest metrics in recall with the type 6 dataset, reaching a peak value of 0.793. Regarding the precision and F1 scores, the DT model using the type 1 dataset demonstrated the strongest results.

Table 4. Non-pretrained model features classification.

Dataset	Model	EMR	Accuracy	Recall	Precision	F1 score
Type 1	DT	0.147	0.638	0.638	**0.683**	**0.639**
	RF	0.163	0.646	0.654	0.645	0.625
	SVM	0.108	0.599	0.593	0.671	0.606
	LSTM	0.115	0.669	0.665	0.487	0.539
	Transformer	0.138	0.628	0.528	0.390	0.412
Type 2	DT	0.123	0.637	0.643	0.669	0.632
	RF	0.165	0.645	0.673	0.616	0.615
	SVM	0.074	0.580	0.577	0.677	0.599
	LSTM	0.156	0.679	0.764	0.537	0.598
	Transformer	0.113	0.631	0.571	0.347	0.394
Type 3	DT	0.148	0.618	0.609	0.677	0.620
	RF	0.165	0.645	0.656	0.612	0.616
	SVM	0.106	0.571	0.559	0.649	0.576
	LSTM	0.156	0.689	0.700	0.501	0.567
	Transformer	0.131	0.617	0.456	0.287	0.323
Type 4	DT	0.115	0.611	0.617	0.665	0.615
	RF	0.164	0.656	0.673	0.640	0.635
	SVM	0.083	0.573	0.575	0.624	0.572
	LSTM	0.132	0.662	0.719	0.499	0.565
	Transformer	0.122	0.624	0.491	0.323	0.362
Type 5	DT	0.106	0.644	0.643	0.663	0.632
	RF	0.147	0.653	0.670	0.641	0.632
	SVM	0.074	0.557	0.542	0.631	0.560
	LSTM	0.124	0.678	0.698	0.496	0.559
	Transformer	0.130	0.610	0.461	0.373	0.394
Type 6	DT	0.107	0.620	0.611	0.679	0.621
	RF	0.147	0.649	0.673	0.604	0.612
	SVM	0.091	0.566	0.566	0.644	0.573
	LSTM	0.115	0.689	**0.793**	0.517	0.604
	Transformer	0.114	0.609	0.486	0.319	0.361
Type 7	DT	0.140	0.615	0.614	0.661	0.614
	RF	0.164	0.651	0.675	0.640	0.631

 doi:10.20944/preprints202401.0941.v1

	SVM	0.090	0.573	0.574	0.645	0.578
	LSTM	0.139	**0.699**	0.776	0.549	0.615
	Transformer	0.131	0.611	0.370	0.348	0.336
Type 8	DT	0.100	0.621	0.612	0.662	0.614
	RF	0.163	0.641	0.656	0.612	0.609
	SVM	0.082	0.554	0.546	0.627	0.558
	LSTM	**0.172**	0.680	0.708	0.487	0.551
	Transformer	0.073	0.611	0.404	0.355	0.344

Underlined values are the best for each dataset, and underlined and bold values are the best overall. Type 1: only before-treatment features; Type 2: before-treatment features with age; Type 3: before-treatment features with sex; Type 4: before-treatment features with day; Type 5: before-treatment features with age and sex; Type 6: before-treatment features with age and day; Type 7: before-treatment features with sex and day; Type 8: before-treatment features with age, sex, and day; EMR: exact match ratio; DT, decision tree; RF, random forest; SVM: support vector machine; LSTM: long short-term memory.

3.4. Pretrained model features classification.

Datasets 6, 7, and 8, which exhibited the highest scores for recall, accuracy, and EMR, respectively, in the non-pretrained model, were selected for the pretrained model evaluation (Table 5). The pretrained model was evaluated only one-fold, and for an intuitive comparison, the non-pretrained model performance shown in Table 5 was a one-fold result selected from the 10-fold data. Across the three datasets, GPT3.5 with prompt engineering, did not achieve an accuracy exceeding 0.5. In contrast, GPT4.0 outperformed GPT3.5 in all evaluation metrics. In the type 8 dataset, the fine-tuned GPT3.5-turbo-1160 model exhibited the most impressive results, whereas its performance on the type 7 dataset was comparatively lower. When focusing on the type 7 dataset, the LSTM model achieved the highest accuracy and recall. However, for the type 8 dataset, GPT4.0 with prompt engineering emerged as a superior model in terms of EMR, precision, and F1 score.

Table 5. Non-pretrained and pretrained model features classification.

Dataset	Model	EMR	Accuracy	Recall	Precision	F1 score
Type 6	DT	0.000	0.637	0.727	0.635	0.672
	RF	0.077	0.637	0.777	0.611	0.669
	SVM	0.077	0.670	0.799	0.646	0.701
	LSTM	0.154	0.681	0.895	0.552	0.655
	Transformer	0.077	0.505	0.552	0.332	0.360
	GPT3.5 (P)	0.077	0.440	0.610	0.330	0.397
	GPT4.0 (P)	0.000	0.615	0.746	0.665	0.674
	GPT3.5-turbo-1160 (F)	0.154	0.527	0.726	0.412	0.503
Type 7	DT	0.077	0.582	0.688	0.593	0.632
	RF	0.154	0.626	0.768	0.585	0.649
	SVM	0.154	0.637	0.783	0.581	0.646
	LSTM	0.154	**0.703**	**0.907**	0.587	0.707
	Transformer	0.000	0.560	0.453	0.563	0.492
	GPT3.5 (P)	0.077	0.396	0.538	0.358	0.416
	GPT4.0 (P)	0.077	0.560	0.667	0.629	0.638
	GPT3.5-turbo-1160 (F)	0.000	0.484	0.593	0.512	0.538

Preprints (www.preprints.org) | NOT PEER-REVIEWED | Posted: 11 January 2024 doi:10.20944/preprints202401.0941.v1

Type 8	DT	0.000	0.637	0.727	0.635	0.672
	RF	0.154	0.626	0.768	0.585	0.649
	SVM	0.077	0.648	0.780	0.599	0.660
	LSTM	**0.231**	0.692	0.781	0.635	0.685
	Transformer	0.000	0.560	0.375	0.571	0.451
	GPT3.5 (P)	0.077	0.407	0.369	0.278	0.246
	GPT4.0 (P)	**0.231**	0.659	0.742	**0.731**	**0.723**
	GPT3.5-turbo-1160 (F)	0.077	0.615	0.714	0.613	0.646

Underlined values are the best for each dataset, and underlined and bold values are the best overall. Type 6: before-treatment features with age and day; Type 7: before-treatment features with sex and day; Type 8: before-treatment features with age, sex, and day; EMR: exact match ratio; DT, decision tree; RF, random forest; SVM: support vector machine; LSTM: long short-term memory; (P): prompt engineering; (F): fine-tuning.

3.5. Stress classification.

Stress classification was binary (Figure 2C). The feature classification result is calculated as a stress score but the stress classification is classified as "yes (> 50%)" or "no (< 50%)" based on the criterion of a stress score of 50%. Therefore, this differs from the feature classification results. As shown in Table 6, among the non-pretrained models, the LSTM using the type 7 dataset achieved the highest accuracy (0.846) in stress classification. For the pretrained models on the type 8 dataset, GPT4.0 with prompt engineering, demonstrated the highest accuracy at 0.769 and GPT3.5 with prompt engineering, had the highest recall at 0.800, but the lowest accuracy at 0.385. The RF and SVM models exhibited equivalent performances across the three types of datasets. The DT and transformer models were the most effective for the type 8 dataset.

Table 6. Non-pretrained and pretrained model stress classification.

Dataset	Model	Accuracy	Recall	Precision	F1 score
Type 6	DT	0.615	0.375	0.429	0.400
	RF	0.769	0.400	0.571	0.471
	SVM	0.769	0.400	0.571	0.471
	LSTM	0.692	0.444	0.500	0.471
	Transformer	0.538	0.571	0.400	0.471
	GPT3.5 (P)	0.385	0.600	0.300	0.400
	GPT4.0 (P)	0.615	0.500	0.444	0.471
	GPT3.5-turbo-1160 (F)	0.615	0.375	0.429	0.400
Type 7	DT	0.615	0.250	0.400	0.308
	RF	0.769	0.400	0.571	0.471
	SVM	0.769	0.400	0.571	0.471
	LSTM	**0.846**	0.364	**0.667**	0.471
	Transformer	0.538	0.571	0.400	0.471
	GPT3.5 (P)	0.462	0.500	0.333	0.400
	GPT4.0 (P)	0.385	0.200	0.167	0.182
	GPT3.5-turbo-1160 (F)	0.462	0.167	0.200	0.182
Type 8	DT	0.692	0.333	0.500	0.400
	RF	0.769	0.400	0.571	0.471
	SVM	0.769	0.400	0.571	0.471

 doi:10.20944/preprints202401.0941.v1

LSTM	0.769	0.400	0.571	0.471
Transformer	0.692	0.000	0.000	0.000
GPT3.5 (P)	0.385	**0.800**	0.333	0.471
GPT4.0 (P)	0.769	0.300	0.600	0.400
GPT3.5-turbo-1160 (F)	0.615	0.250	0.400	0.308

Underlined values are the best for each dataset, and underlined and bold values are the best overall. Type 6: before-treatment features with age and day; Type 7: before-treatment features with sex and day; Type 8: before-treatment features with age, sex, and day; EMR: exact match ratio; DT, decision tree; RF, random forest; SVM: support vector machine; LSTM: long short-term memory; (P): prompt engineering; (F): fine-tuning.

4. Discussion

Stress in patients undergoing radiation therapy can lead to muscle stiffness, affecting treatment setup accuracy, and potentially causing accidents due to movement or falls. Although posttreatment surveys have validated stress in patients undergoing radiation therapy, in-room stress during treatment remains unmeasured. Our study, utilizing biological signals, revealed that 90% of patients experienced stress during treatment. Our research enables the identification of cancer patients undergoing radiation therapy who require interventions to reduce stress before treatment. By recognizing and mitigating stress in advance, the accuracy of radiation therapy can be enhanced, ultimately improving treatment outcomes.

Table 2 presents the distribution of the during-treatment stress scores measured using biological signals from 41 patients. Of the 123 stress cases, 12 (9.76%) showed no stress, while 111 (90.24%) indicated stress. The highest stress score distribution (85.71%) was observed in 26 patients (21.14%). The evaluation of the presence of stress based on a 50% stress score threshold was 47.15%. In [55], it was found that 21-54% of patients undergoing radiation therapy experienced stress. This range encompasses our findings, where using a 50% stress score as a threshold, we observed that 47.15% of the cases involved stress.

Figure 3 shows the variation in patients' stress scores over different days. For males, the stress scores on days one and two were similar, exceeding 50% on day three and remaining similar on day four. In females, there was a slight increase on day two, a decrease on day three, and a significant decrease on day four. Overall, except for day two, males exhibited higher stress scores than females on all dates. Furthermore, males exhibited an increasing trend in stress as treatment progressed, whereas females showed a decreasing trend. However, the stress score trends did not show a statistical significance. In [56], it was indicated that female stress decreased over the course of treatment, whereas male stress did not change significantly. Although not statistically significant, our study's stress score trends showed tendencies similar to those of other research findings.

Implementing pre-treatment measures to reduce stress is challenging for all patients. When calculating the stress using a threshold of 50% stress score, 47.15% of the cases exhibited stress. Studies [35] and [56] found that factors such as age, occupation, marital status, and gender differences do not significantly affect stress. While our study found higher initial stress in females, the overall stress scores were higher in males. Considering the referenced studies and our research, it may be inaccurate to select specific patient groups for before treatment stress-reduction measures. Therefore, it is necessary to predict stress in all patients prior to treatment.

Our study utilized five non-pretrained models and eight dataset types to classify changes in the features during treatment (Table 4). The RF model exhibited the best overall EMR across the datasets, and the LSTM model had the highest EMR of 0.172 for the type 8 dataset. The LSTM performed best in terms of accuracy across all datasets, particularly in the type 7 dataset, with an accuracy of 0.699. Similarly, LSTM had the highest recall across all datasets. The DT model had the highest precision and F1 scores of 0.683 and 0.639, respectively. In predictive modeling, accurately identifying actual stress states is crucial, rather than mislabeling non-stressed individuals as stressed. Hence, Types 6,

 doi:10.20944/preprints202401.0941.v1

7, and 8 datasets, which exhibited the highest recall, accuracy, and EMR, respectively, were selected to evaluate the pretrained model using one-fold data.

In the analysis presented in Table 5, for the type 6 and type 7 datasets, the LSTM model continued to outperform the others in terms of EMR, accuracy, and recall, which is consistent with the findings in Table 4. However, in the type 8 dataset, both GPT4.0 and LSTM demonstrated superior performance in EMR, achieving a score of 0.231. While LSTM led to accuracy and recall, GPT4.0 excelled in precision and F1 score. GPT3.5 displayed the lowest performance across all indicators in these datasets, with GPT3.5-turbo-1160 achieving an accuracy of 0.615 for the type 8 dataset.

Considering all models, including non-pretrained and pretrained, the LSTM model demonstrated robust performance across all evaluation indices and datasets, making it the most suitable for feature classification during treatment. In scenarios where implementing a machine learning model is challenging, the pretrained GPT4.0 model, particularly with the type 8 dataset, emerged as the most appropriate choice.

Stress classification classifies “yes (> 50%)” or “no (< 50%)” based on the criterion of stress score of 50% (Table 6). In stress classification, the LSTM of the type 7 dataset classified stress effectively with an accuracy of 0.846. The RF and SVM exhibited a stability of 0.769 accuracy across all datasets. For the pretrained model, GPT4.0 showed an accuracy of 0.769 in the type 8 dataset that included all data, but in the type 7 dataset, all pretrained models failed to exceed the accuracy of 0.5. As with feature classification, LSTM was the best among all models for stress classification, with GPT4.0 being superior for the type 8 dataset. GPT4.0 is suited for predictions using diverse patient information, whereas LSTM is recommended because of its stability in scenarios with limited information.

Datasets 6, 7, and 8 used for comparison in Tables 5 and 6 contain the treatment days. The treatment day is important information for stress prediction. The performance of the non-pretrained model was similar across the three dataset types. However, the pretrained model performance was the best in the type 8 dataset, which included age, sex, and treatment day, and the worst in the type 7 dataset, in which age was omitted. Stress prediction using a pre-trained model may be better when using all available patient information.

Our study is pioneering in the use of before-treatment information to predict during-treatment stress, in contrast to most studies that have focused on current stress. In [57], the predicted stress in surveys using biological signals such as respiration, ECG, and electrodermal activity showed an accuracy of 86%, and [58] used ECG and neural networks to predict survey stress with 85% accuracy. A few studies have predicted future stress levels. In [59], the driver's breathing, ECG, and galvanic skin response signals in real-time were used to predict stress after one minute with 94% accuracy. In [60], signals, such as the participant's 24-hour physiology, weather, number of calls, and location, were used to predict the next day's mood with an accuracy of 82.2%. Although a direct comparison with these studies is difficult, in our study, the LSTM using the type 7 dataset showed an accuracy of 84.6%. The accuracy of our research in predicting future information and HRV information obtained through limited PPG was sufficiently high, and we believe that the addition of learning datasets and patient biological signals will result in even higher accuracy.

This study has certain limitations. This study focused on patients with lung cancer who underwent their first radiation therapy session. The use of finger-worn sensors did not affect therapy for patients with lung cancer. However, the limited methods for measuring biological signals and the narrow patient population have resulted in restricted participant diversity and a lack of standardization in stress assessment methods. Expanding the research to include various cancer patients using sensor technologies that do not interfere with treatment could enhance the accuracy of stress prediction and enable more precise evaluations. Although AI-based stress prediction using biological signals has demonstrated over 80% accuracy, the impact of the measured stress score on the actual radiation therapy remains unverified. Further research is required to analyze the correlations between stress indicators and variables related to treatment accuracy, such as patient breathing, couch positioning, and setup times. Assigning weights to features with a high correlation could lead to more accurate stress assessments. Future research will aim to select appropriate sensor

 doi:10.20944/preprints202401.0941.v1

technologies, involve diverse cancer patient groups, and explore the relationship between stress and radiation therapy outcomes.

5. Conclusions

This study marks a significant advancement in cancer radiation therapy by employing AI and biological signals for stress prediction. This highlights the potential use of these tools in identifying patients who may require psychological support prior to treatment. This study suggests the need for more diverse biological signals and patient groups to enhance our understanding of the effects of stress on radiation therapy.

Author Contributions: Conceptualization, Y. H. (Youngyih Han); Methodology, S. J. (Sangwoon Jeong); Software, S. J.; Validation, S. J. and Y. H.; Formal analysis, S. J.; Investigation, S. J.; Resources, H. P. (Hongryull Pyo) and W. P. (Won Park). Data curation: S.J.; Writing-original draft preparation: S.J.; Writing-review and editing: S.J. and Y.H.; Visualization: S.J.; Supervision: Y.H.; Project administration: Y.H.; Funding acquisition: Y.H.

Funding: This research was supported by the National Research Foundation of Korea grant funded by the Korean government (MSIT) 2022R1A2C2004694.

Institutional Review Board Statement: The study was conducted in accordance with the Declaration of Helsinki and approved by the Institutional Review Board of the Samsung Medical Center (IRB number 2020-11-162).

Informed Consent Statement: Informed consent was obtained from all participants involved in the study.
Data Availability Statement: The datasets used in this study are available from the corresponding author upon reasonable request.

Conflicts of Interest: The authors declare no conflict of interest.

References

1. Siegel, R.L.; Miller, K.D.; Wagle, N.S.; Jemal, A. Cancer statistics, 2023. *Ca Cancer J Clin* **2023**, *73*, 17-48.
2. Baskar, R.; Lee, K.A.; Yeo, R.; Yeoh, K.-W. Cancer and radiation therapy: current advances and future directions. *International journal of medical sciences* **2012**, *9*, 193.
3. Abshire, D.; Lang, M.K. The evolution of radiation therapy in treating cancer. In Proceedings of the Seminars in oncology nursing, 2018; pp. 151-157.
4. Van Herk, M. Errors and margins in radiotherapy. In Proceedings of the Seminars in radiation oncology, 2004; pp. 52-64.
5. Rudat, V.; Flentje, M.; Oetzel, D.; Menke, M.; Schlegel, W.; Wannenmacher, M. Influence of the positioning error on 3D conformal dose distributions during fractionated radiotherapy. *Radiotherapy and Oncology* **1994**, *33*, 56-63.
6. Fu, W.; Yang, Y.; Yue, N.J.; Heron, D.E.; Huq, M.S. Dosimetric influences of rotational setup errors on head and neck carcinoma intensity-modulated radiation therapy treatments. *Medical Dosimetry* **2013**, *38*, 125-132.
7. Siebers, J.V.; Keall, P.J.; Wu, Q.; Williamson, J.F.; Schmidt-Ullrich, R.K. Effect of patient setup errors on simultaneously integrated boost head and neck IMRT treatment plans. *International Journal of Radiation Oncology* Biology* Physics* **2005**, *63*, 422-433.
8. Tsujii, K.; Ueda, Y.; Isono, M.; Miyazaki, M.; Teshima, T.; Koizumi, M. Dosimetric impact of rotational setup errors in volumetric modulated arc therapy for postoperative cervical cancer. *Journal of Radiation Research* **2021**, *62*, 688-698.
9. Van Dyk, J.; Battista, J.J.; Bauman, G.S. Accuracy and uncertainty considerations in modern radiation oncology. *The modern technology of radiation oncology* **2013**, *3*, 361-412.
10. Huang, G.; Medlam, G.; Lee, J.; Billingsley, S.; Bissonnette, J.-P.; Ringash, J.; Kane, G.; Hodgson, D.C. Error in the delivery of radiation therapy: results of a quality assurance review. *International Journal of Radiation Oncology* Biology* Physics* **2005**, *61*, 1590-1595.
11. Huq, M.S.; Fraass, B.A.; Dunscombe, P.B.; Gibbons Jr, J.P.; Ibbott, G.S.; Mundt, A.J.; Mutic, S.; Palta, J.R.; Rath, F.; Thomadsen, B.R. The report of Task Group 100 of the AAPM: Application of risk analysis methods to radiation therapy quality management. *Medical physics* **2016**, *43*, 4209-4262.
12. Wu, Q.J.; Thongphiew, D.; Wang, Z.; Chankong, V.; Yin, F.F. The impact of respiratory motion and treatment technique on stereotactic body radiation therapy for liver cancer. *Medical physics* **2008**, *35*, 1440-1451.

13. Yamashita, H.; Haga, A.; Hayakawa, Y.; Okuma, K.; Yoda, K.; Okano, Y.; Tanaka, K.-i.; Imae, T.; Ohtomo, K.; Nakagawa, K. Patient setup error and day-to-day esophageal motion error analyzed by cone-beam computed tomography in radiation therapy. *Acta Oncologica* **2010**, *49*, 485-490.
14. Poroch, D. The effect of preparatory patient education on the anxiety and satisfaction of cancer patients receiving radiation therapy. *Cancer Nursing* **1995**, *18*, 206-214.
15. Keall, P.J.; Mageras, G.S.; Balter, J.M.; Emery, R.S.; Forster, K.M.; Jiang, S.B.; Kapatoes, J.M.; Low, D.A.; Murphy, M.J.; Murray, B.R. The management of respiratory motion in radiation oncology report of AAPM Task Group 76 a. *Medical physics* **2006**, *33*, 3874-3900.
16. Lee, H.; Ahn, Y.C.; Oh, D.; Nam, H.; Noh, J.M.; Park, S.Y. Tumor volume reduction rate during adaptive radiation therapy as a prognosticator for nasopharyngeal cancer. *Cancer Research and Treatment: Official Journal of Korean Cancer Association* **2016**, *48*, 537-545.
17. Woodford, C.; Yartsev, S.; Dar, A.R.; Bauman, G.; Van Dyk, J. Adaptive radiotherapy planning on decreasing gross tumor volumes as seen on megavoltage computed tomography images. *International Journal of Radiation Oncology* Biology* Physics* **2007**, *69*, 1316-1322.
18. Grassi, G.; Vailati, S.; Bertinieri, G.; Seravalle, G.; Stella, M.L.; Dell'Oro, R.; Mancia, G. Heart rate as marker of sympathetic activity. *Journal of hypertension* **1998**, *16*, 1635-1639.
19. Fisher, J.; Paton, J. The sympathetic nervous system and blood pressure in humans: implications for hypertension. *Journal of human hypertension* **2012**, *26*, 463-475.
20. Roman-Liu, D.; Grabarek, I.; Bartuzi, P.; Choromański, W. The influence of mental load on muscle tension. *Ergonomics* **2013**, *56*, 1125-1133.
21. Lundberg, U.; Frankenhaeuser, M. Stress and workload of men and women in high-ranking positions. *Journal of occupational health psychology* **1999**, *4*, 142.
22. Van Hasselt, V.B.; Sheehan, D.C.; Malcolm, A.S.; Sellers, A.H.; Baker, M.T.; Couwels, J. The law enforcement officer stress survey (LEOSS) evaluation of psychometric properties. *Behavior modification* **2008**, *32*, 133-151.
23. Prasad, K.; McLoughlin, C.; Stillman, M.; Poplau, S.; Goelz, E.; Taylor, S.; Nankivil, N.; Brown, R.; Linzer, M.; Cappelucci, K. Prevalence and correlates of stress and burnout among US healthcare workers during the COVID-19 pandemic: a national cross-sectional survey study. *EClinicalMedicine* **2021**, *35*.
24. Oh, H.-M.; Son, C.-G. The risk of psychological stress on cancer recurrence: A systematic review. *Cancers* **2021**, *13*, 5816.
25. De Jaeghere, E.A.; Kanervo, H.; Colman, R.; Schrauwen, W.; West, P.; Vandemaele, N.; De Pauw, A.; Jacobs, C.; Hilderson, I.; Saerens, M. Mental health and quality of life among patients with cancer during the SARS-CoV-2 pandemic: results from the longitudinal ONCOVID survey study. *Cancers* **2022**, *14*, 1093.
26. Skwirczyńska, E.; Chudecka-Głaz, A.; Wróblewski, O.; Tejchman, K.; Skonieczna-Żydecka, K.; Piotrowiak, M.; Michalczyk, K.; Karakiewicz, B. Age Matters: The Moderating Effect of Age on Styles and Strategies of Coping with Stress and Self-Esteem in Patients with Neoplastic Prostate Hyperplasia. *Cancers* **2023**, *15*, 1450.
27. Scherpenzeel, A.C.; Saris, W.E. The validity and reliability of survey questions: A meta-analysis of MTMM studies. *Sociological Methods & Research* **1997**, *25*, 341-383.
28. Vinkers, C.H.; Penning, R.; Hellhammer, J.; Verster, J.C.; Klaessens, J.H.; Olivier, B.; Kalkman, C.J. The effect of stress on core and peripheral body temperature in humans. *Stress* **2013**, *16*, 520-530.
29. McDuff, D.J.; Hernandez, J.; Gontarek, S.; Picard, R.W. Cogcam: Contact-free measurement of cognitive stress during computer tasks with a digital camera. In Proceedings of the Proceedings of the 2016 CHI Conference on Human Factors in Computing Systems, 2016; pp. 4000-4004.
30. Krantz, G.; Forsman, M.; Lundberg, U. Consistency in physiological stress responses and electromyographic activity during induced stress exposure in women and men. *Integrative Physiological & Behavioral Science* **2004**, *39*, 105-118.
31. Mohan, P.M.; Nagarajan, V.; Das, S.R. Stress measurement from wearable photoplethysmographic sensor using heart rate variability data. In Proceedings of the 2016 International Conference on Communication and Signal Processing (ICCSP), 2016; pp. 1141-1144.
32. Salahuddin, L.; Kim, D. Detection of acute stress by heart rate variability using a prototype mobile ECG sensor. In Proceedings of the 2006 International Conference on Hybrid Information Technology, 2006; pp. 453-459.
33. Punita, P.; Saranya, K.; Kumar, S.S. Gender difference in heart rate variability in medical students and association with the level of stress. *National Journal of Physiology, Pharmacy and Pharmacology* **1970**, *6*, 431-431.
34. Dai, R.; Lu, C.; Yun, L.; Lenze, E.; Avidan, M.; Kannampallil, T. Comparing stress prediction models using smartwatch physiological signals and participant self-reports. *Computer Methods and Programs in Biomedicine* **2021**, *208*, 106207.
35. Antoni, D.; Vigneron, C.; Clavier, J.-B.; Guihard, S.; Velten, M.; Noel, G. Anxiety during radiation therapy: a prospective randomized controlled trial evaluating a specific one-on-one procedure announcement provided by a radiation therapist. *Cancers* **2021**, *13*, 2572.

36. Lewis, F.; Merckaert, I.; Liénard, A.; Libert, Y.; Etienne, A.-M.; Reynaert, C.; Slachmuylder, J.-L.; Scalliet, P.; Coucke, P.; Salamon, E. Anxiety and its time courses during radiotherapy for non-metastatic breast cancer: a longitudinal study. *Radiotherapy and Oncology* **2014**, *111*, 276-280.
37. Cinaz, B.; Arnrich, B.; La Marca, R.; Tröster, G. Monitoring of mental workload levels during an everyday life office-work scenario. *Personal and ubiquitous computing* **2013**, *17*, 229-239.
38. Clays, E.; De Bacquer, D.; Crasset, V.; Kittel, F.; De Smet, P.; Kornitzer, M.; Karasek, R.; De Backer, G. The perception of work stressors is related to reduced parasympathetic activity. *International archives of occupational and environmental health* **2011**, *84*, 185-191.
39. Hynynen, E.; Konttinen, N.; Kinnunen, U.; Kyröläinen, H.; Rusko, H. The incidence of stress symptoms and heart rate variability during sleep and orthostatic test. *European journal of applied physiology* **2011**, *111*, 733-741.
40. Lucini, D.; Norbiato, G.; Clerici, M.; Pagani, M. Hemodynamic and autonomic adjustments to real life stress conditions in humans. *Hypertension* **2002**, *39*, 184-188.
41. Taelman, J.; Vandeput, S.; Vlemincx, E.; Spaepen, A.; Van Huffel, S. Instantaneous changes in heart rate regulation due to mental load in simulated office work. *European journal of applied physiology* **2011**, *111*, 1497-1505.
42. Tharion, E.; Parthasarathy, S.; Neelakantan, N. Short-term heart rate variability measures in students during examinations. *Natl Med J India* **2009**, *22*, 63-66.
43. Visnovcova, Z.; Mestanik, M.; Javorka, M.; Mokra, D.; Gala, M.; Jurko, A.; Calkovska, A.; Tonhajzerova, I. Complexity and time asymmetry of heart rate variability are altered in acute mental stress. *Physiological measurement* **2014**, *35*, 1319.
44. Madden, K.; Savard, G. Effects of mental state on heart rate and blood pressure variability in men and women. *Clinical Physiology* **1995**, *15*, 557-569.
45. Arsalan, A.; Anwar, S.M.; Majid, M. Mental stress detection using data from wearable and non-wearable sensors: a review. *arXiv preprint arXiv:2202.03033* **2022**.
46. Castaldo, R.; Melillo, P.; Bracale, U.; Caserta, M.; Triassi, M.; Pecchia, L. Acute mental stress assessment via short term HRV analysis in healthy adults: A systematic review with meta-analysis. *Biomedical Signal Processing and Control* **2015**, *18*, 370-377.
47. Karthikeyan, P.; Murugappan, M.; Yaacob, S. Detection of human stress using short-term ECG and HRV signals. *Journal of Mechanics in Medicine and Biology* **2013**, *13*, 1350038.
48. Quinlan, J.R. Learning decision tree classifiers. *ACM Computing Surveys (CSUR)* **1996**, *28*, 71-72.
49. Liaw, A.; Wiener, M. Classification and regression by randomForest. *R news* **2002**, *2*, 18-22.
50. Gunn, S.R. Support vector machines for classification and regression. *ISIS technical report* **1998**, *14*, 5-16.
51. Hochreiter, S.; Schmidhuber, J. Long short-term memory. *Neural computation* **1997**, *9*, 1735-1780.
52. Vaswani, A.; Shazeer, N.; Parmar, N.; Uszkoreit, J.; Jones, L.; Gomez, A.N.; Kaiser, Ł.; Polosukhin, I. Attention is all you need. *Advances in neural information processing systems* **2017**, *30*.
53. Lester, B.; Al-Rfou, R.; Constant, N. The power of scale for parameter-efficient prompt tuning. *arXiv preprint arXiv:2104.08691* **2021**.
54. Ziegler, D.M.; Stiennon, N.; Wu, J.; Brown, T.B.; Radford, A.; Amodei, D.; Christiano, P.; Irving, G. Fine-tuning language models from human preferences. *arXiv preprint arXiv:1909.08593* **2019**.
55. Stiegelis, H.E.; Ranchor, A.V.; Sanderman, R. Psychological functioning in cancer patients treated with radiotherapy. *Patient Education and Counseling* **2004**, *52*, 131-141.
56. Irwin, P.; Kramer, S.; Diamond, N.H.; Malone, D.; Zivin, G. Sex differences in psychological distress during definitive radiation therapy for cancer. *Journal of Psychosocial Oncology* **1986**, *4*, 63-75.
57. Gazi, A.H.; Lis, P.; Mohseni, A.; Ompi, C.; Giuste, F.O.; Shi, W.; Inan, O.T.; Wang, M.D. Respiratory markers significantly enhance anxiety detection using multimodal physiological sensing. In Proceedings of the 2021 IEEE EMBS International Conference on Biomedical and Health Informatics (BHI), 2021; pp. 1-4.
58. Vulpe-Grigoraşi, A.; Grigore, O. A neural network approach for anxiety detection based on ECG. In Proceedings of the 2021 International Conference on e-Health and Bioengineering (EHB), 2021; pp. 1-4.
59. Clark, J.; Nath, R.K.; Thapliyal, H. Machine learning based prediction of future stress events in a driving scenario. In Proceedings of the 2021 IEEE 7th World Forum on Internet of Things (WF-IoT), 2021; pp. 455-458.
60. Taylor, S.; Jaques, N.; Nosakhare, E.; Sano, A.; Picard, R. Personalized multitask learning for predicting tomorrow's mood, stress, and health. *IEEE Transactions on Affective Computing* **2017**, *11*, 200-213.